

# Semi-Lumped Compact Low-Pass Filter for Harmonics Suppression

Rui Li · Dong Il Kim · Chang-Mook Choi

## Abstract

In this paper, a new semi-lumped low-pass filter with three finite attenuation poles at stopband is presented. The new structure is composed of a pair of symmetrical parallel coupled-line and a shunted capacitor. With this configuration, three finite attenuation poles can be available for 2nd, 3rd, and 4th harmonics suppression. The research method is based on transmission-line model for tuning the attenuation poles. In order to examine the feasibility of the proposed structure, a low-pass filter based on microstrip structure with harmonics suppression is designed, fabricated, and measured. The experimental results of the fabricated circuit agree well with the simulation and analytical ones.

**Key words** : Finite Attenuation Poles, Harmonics Suppression, Low-Pass Filter, Parallel Coupled-Line.

## I . Introduction

In many communication systems such as mobile and radar systems, the low-pass filters are often employed to suppress harmonics and spurious signals, with the demand for compact size, low insertion loss, and high attenuation. The conventional low-pass filters, such as open-stub low-pass filters and stepped-impedance low-pass filters can not meet the requirements for modern communication systems because of their large size and narrow stopband. For sharp cutoff and high attenuation at stopband, the order of the stepped-impedance low-pass filter must be very high<sup>[1],[2]</sup>, thereby the circuit size and insertion loss will be increased. In literature, many design approaches have been proposed to improve the low-pass filter's performance. The low-pass filters using PBG and DGS structures<sup>[3],[4]</sup> can improve the skirt characteristics and provide wide and deep stopband as compared with the conventional low-pass filters. A low-pass filter using multiple cascaded hairpin resonators that can provide a very sharp cutoff frequency response with low passband insertion loss was demonstrated in [5], [6]. However, this type of design approach is a little complicated and just used to synthesize some parts of available prototype low-pass filters.

In this paper, a new semi-lumped compact low-pass filter with three finite attenuation poles at stopband is proposed. This new type of low-pass filter based on microstrip structure, which consists of a pair of symmetrical parallel coupled-line and a shunted capacitor, is designed. Compared with the conventional low-pass filter, the proposed one demonstrates some attractive

features: simple and compact structure, sharp skirt characteristics, and harmonics suppression.

## II . Finite Attenuation Poles Analysis

Fig. 1 shows the basic layout of the proposed compact low-pass filter. It consists of a shunted capacitor  $C_S$  and a pair of symmetrical parallel coupled-line with a length of  $l_c$ .  $Z_{oe}$  and  $Z_{oo}$  represent the even-and odd-mode characteristic impedances of the parallel coupled-line, respectively.

We assume that the structure is lossless and the width of the feeding lines is negligible. Under these assumptions, the proposed structure can be divided into two sections: one is shunted capacitor section and the other is symmetrical parallel coupled-line section with its far end shorted. As shown in Fig. 2(a), the total Z-matrix of a

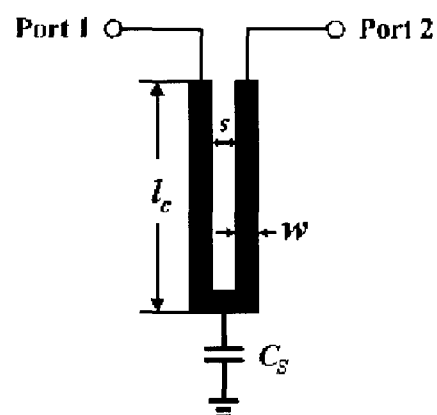


Fig. 1. Proposed semi-lumped compact low-pass filter.

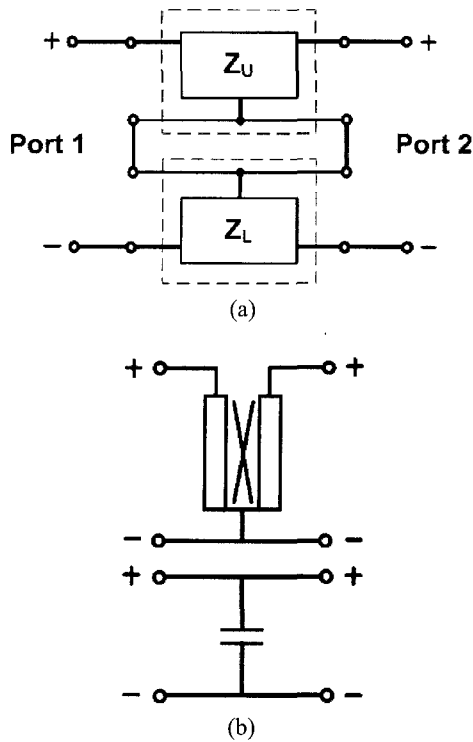


Fig. 2. (a) Serially connected two-port network, (b) Decomposition diagram of the proposed structure.

serially connected network can be given by<sup>[2]</sup>

$$[Z_T] = [Z_U] + [Z_L] \tag{1}$$

where  $[Z_U]$  and  $[Z_L]$  are the impedance matrices of the upper and lower networks, respectively.

As depicted in Fig. 2(b), the coupled-line and shunted capacitor sections can be seen as the upper and lower networks, respectively. For the upper network, the elements of the impedance matrix  $[Z_U]$  can be calculated by using even-odd mode analysis method as followings:

$$Z_{11}^U = j(Z_{oe}\tan\theta_e + Z_{oo}\tan\theta_o)/2 \tag{2a}$$

$$Z_{21}^U = j(Z_{oe}\tan\theta_e - Z_{oo}\tan\theta_o)/2 \tag{2b}$$

For the lower network, the elements of the impedance matrix  $[Z_L]$  are the same and can be derived as:

$$Z_{mn}^L = -j/(\omega C_s), \quad m, n = 1, 2 \tag{3}$$

From the relationship between the impedance and scattering matrices, the transmission coefficient of the network can be obtained by<sup>[7]</sup>

$$S_{21} = \frac{2Z_{12}^T Z_0}{(Z_{11}^T + Z_0)(Z_{22}^T + Z_0) - Z_{12}^T Z_{21}^T} \tag{4}$$

where  $Z_0$  is the characteristic impedance of the input and output microstrip line. The finite attenuation poles are located at the angular frequencies  $\omega$  where  $S_{21}(\omega)$

$=0$  or  $Z_{21}(\omega)=0$ . Therefore, the frequencies of the finite attenuation poles should satisfy the following equation derived from Eqs. (2b) and (3):

$$(Z_{oe}\tan\theta_e - Z_{oo}\tan\theta_o)/2 = 1/(\omega C_s) \tag{5}$$

Inspecting Eq. (5), the frequencies of the finite attenuation poles can be determined by the capacitive load  $C_s$  and the electrical parameters of the parallel coupled-line. Fig. 3(a) shows the pictorial descriptions of varying the capacitance  $C_s$ . There are three intersections between the upper reactance function  $X_U$  and the lower one  $X_L$  through the stopband. It means that three finite attenuation poles will appear through the stopband at the same frequencies as the intersections between the upper and lower reactance functions. As illustrated in Fig. 3(b),

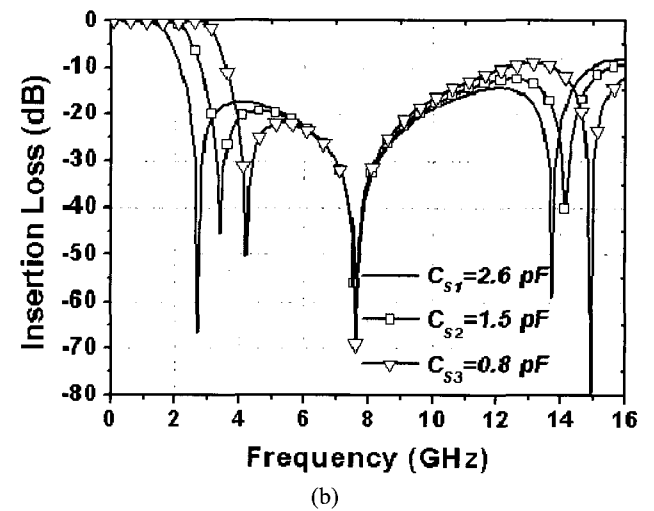
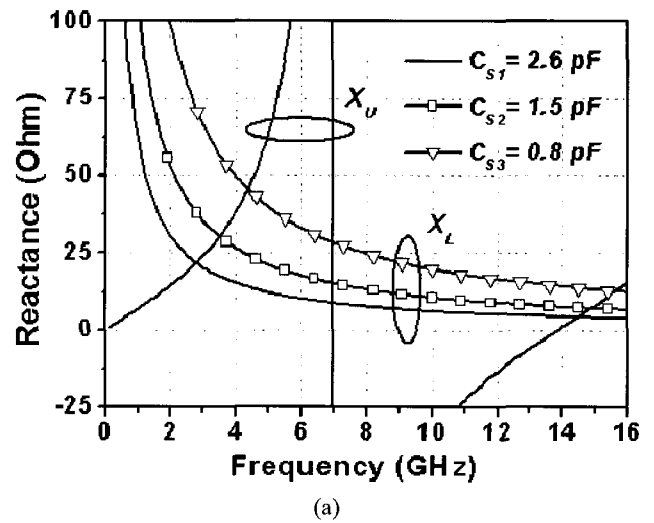


Fig. 3. Compact structure with different capacitive loads. (a) Pictorial reactance descriptions. (b) Simulated frequency responses with the following electrical parameters:  $l_c=7.0$  mm,  $s=0.5$  mm, and  $w=0.23$  mm.

the predicted results are confirmed by the simulated frequency responses. The locations of the transmission zeros are almost same as those of the intersections shown in Fig. 3(a). The simulated results with three different capacitance values demonstrate that the first and third finite attenuation poles shift to the upper frequency as the capacitance value decreases and the second finite attenuation pole has almost no-shift. Moreover, the slope factor of the cut-off transition is about the same. Therefore, the cut-off frequency can be adjusted easily by selecting an appropriate capacitive load without changing the sharpness of the cut-off. The first and second finite attenuation poles, however, will be so close as to produce just one transmission zero when the capacitance value is selected to be small enough. To continuously inspect the effects on the frequency responses of the proposed structure caused by the parallel coupled-line, a comparison has been made among three different structures with different length of the parallel coupled-line based on same capacitive load. As shown in Fig. 4(a), all three intersections shift to the upper frequency as the length of the coupled-line decreases gradually, especially the second and third ones. The frequency responses demonstrated in Fig. 4(b) also present the same characteristics.

### III. Low-Pass Filter Design for Harmonics Suppression

By the above graphic analysis, the proposed compact structure can provide a wide rejection band with three finite attenuation poles, and these finite attenuation poles can be adjusted easily just by changing the capacitive load value and the length of the coupled-line. This attractive feature can be used to improve harmonics and spurious suppression performance. To verify the proposed approach, a low-pass filter unit with its cutoff frequency at 1.3 GHz is developed. The electrical parameters of the parallel coupled-line and shunted capacitor are selected to suppress the 2nd, 3rd, and 4th harmonics, simultaneously. A compact low-pass filter is designed and fabricated on a 0.76 mm thickness Taconic PCB with a relative dielectric constant of  $\epsilon_r=3.5$ . Adjusting the locations of the reactance intersection points by changing the circuit parameters, as well as optimized by Agilent ADS software, the circuit electrical parameters are determined as shown in Table 1, and a comparison of the circuit layouts between the proposed compact low-pass filter and the conventional stepped-impedance one has been made as illustrated in Fig. 5.

A photograph of the fabricated low-pass filter is shown in Fig. 6(a) and the circuit was measured with

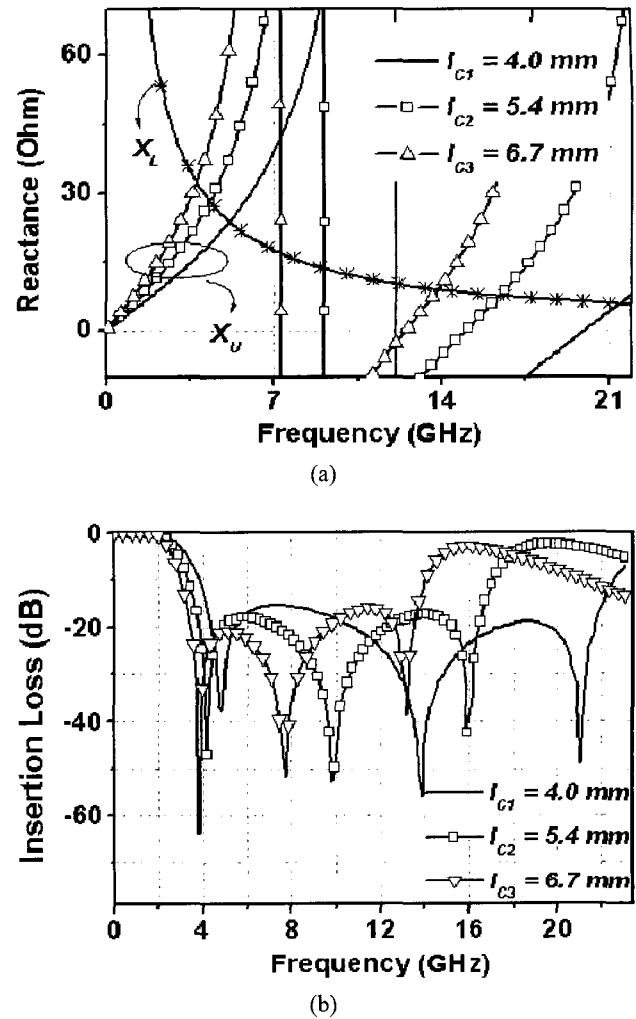


Fig. 4. Compact structure with different length of the parallel coupled-line. (a) Pictorial reactance descriptions. (b) Simulated frequency responses with the following electrical parameters:  $C_S=1.3$  pF,  $s=0.5$  mm, and  $w=0.23$  mm.

Table 1. Comparison of the physical dimensions.

Proposed LPF		Stepped-impedance LPF	
Coupled-line (mm)	Capacitor (pF)	High-impedance line (mm)	Low-impedance line (mm)
Length: 13	$C_S: 1.5$	Length: 11.51	Length: 8.45
Width: 0.4		Width: 0.22	Width: 4.54
Space: 0.4			
Substrate thickness: 0.76 mm, relative dielectric: 3.5			

Anritsu 37369D vector network analyzer. As shown in Fig. 6(b), the measured results agree well with the simulated ones. This low-pass filter has a 3-dB cutoff frequency at 1.3 GHz. The three finite attenuation poles at stopband are located at 2.7 GHz, 3.85 GHz, and 5.35

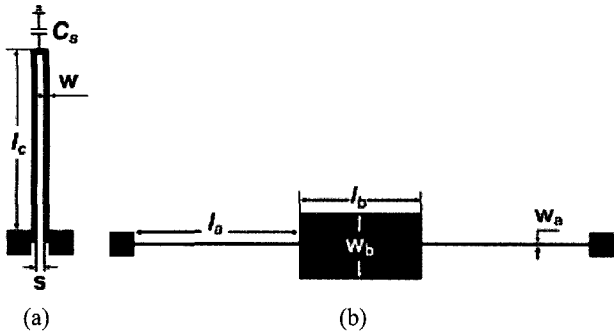


Fig. 5. Layouts of (a) the proposed low-pass filter and (b) conventional stepped-impedance low-pass filter.

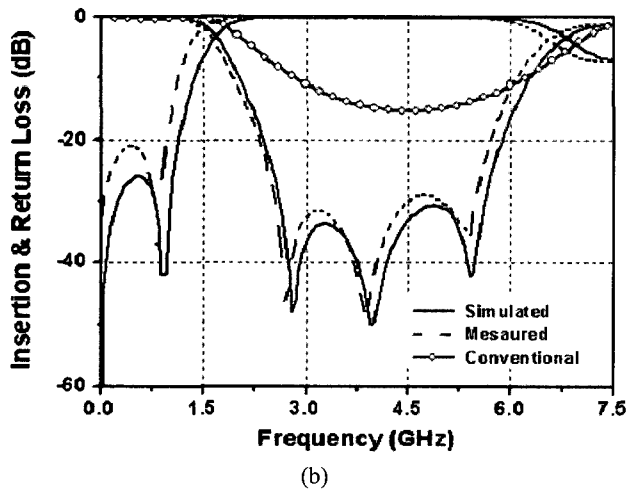
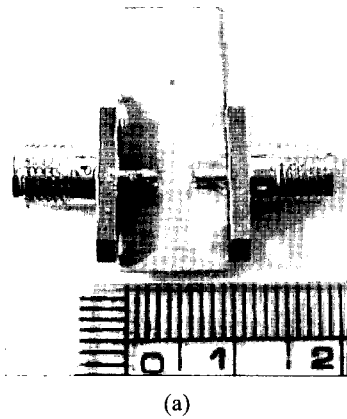


Fig. 6. Proposed compact low-pass filter. (a) Photograph of the fabricated circuit, (b) Measured frequency responses compared with those of the simulated and conventional stepped-impedance low-pass filter.

GHz with insertion losses of 46 dB, 47.9 dB, and 35.5 dB, respectively. The locations are almost same as the 2nd, 3rd, and 4th harmonics of the cutoff frequency. Thereby the harmonics can be eliminated effectively.

#### IV. Conclusions

A new compact low-pass filter with three finite attenuation poles at stopband has been developed in this paper. Through theoretical analysis and simulation performance, the rejection band can be controlled by adjusting the circuit electrical parameters. To verify the feasibility of the proposed method, a low-pass filter unit has been designed, fabricated, and measured. Based on our observations of simulation performance and measured results, this new type of low-pass filter demonstrates some desirable features compared with the conventional one, such as sharp skirt characteristics and harmonics and spurious suppression at stopband. In addition, the proposed approach can be further extended and used in high-order design process to achieve sharper skirt characteristics and a broad rejection band with much deeper attenuation level.

This work was supported by the Korea Research Foundation Grant (KRF-2005-005-J00502).

#### References

- [1] G. L. Mattaei, L. Young, and E. M. T. Jones, *Microwave Filters, Impedance Matching Networks and Coupling Structure*, New York: McGraw-Hill, 1980.
- [2] Jia-Sheng Hong, M. J. Lancaster, *Microstrip Filters for RF/Microwave Applications*, New York: John Wiley & Sons, 2001.
- [3] I. Rumsey, M. Picket-May, and P. K. Kelly, "Photonic bandgap structure used as filters in microstrip circuits", *IEEE Microw. Guided Wave Lett.*, vol. 8, no. 10, pp. 336-338, Oct. 1998.
- [4] D. Ahn, J. S. Park, C. S. Kim, J. Kim, Y. Qian, and T. Itoh, "A design of the low-pass filter using the novel microstrip defected ground structure", *IEEE Trans. Microw. Theory Tech.*, vol. 49, no. 1, pp. 86-93, Jan. 2001.
- [5] L-H Hsieh, K. Chang, "Compact low-pass filter using stepped impedance hairpin resonator", *Electron. Lett.*, vol. 37, no. 14, pp. 899-900, Jul. 2001.
- [6] L-H Hsieh, K. Chang, "Compact elliptic-function low-pass filters using microstrip stepped-impedance hairpin resonators", *IEEE Microw. Theory Tech.*, vol. 51, no. 1, pp. 193-199, Jan. 2003.
- [7] David M. Pozar, *Microwave Engineering, 3rd*, New York: John Wiley & Sons, 2005.

Rui Li



He received his B.S. degree in electrical engineering from Hebei University of Science & Technology, Shijiazhuang, China, in 2001, and his M.S. degree in radio sciences & engineering from Korea Maritime University, Busan, Korea, in 2005, and is currently working toward the Ph.D. degree in radio sciences & engineering at Korea Maritime University, Busan, Korea. His research interests include microwave integrated circuit and RF devices, and EMC/EMI countermeasures.

Chang-Mook Choi



He received the B.E. degree from Korea Naval Academy in 1996 and M.E degree from AIMST in 2001. He is currently working toward the Ph.D. degree in department of radio science & engineering at Korea Maritime University. His research interests include the development of EM wave absorber, EMI/EMC, and navigation systems.

Dong Il Kim



He received his B.E. and M.E. degrees in nautical science and electronic communications from Korea Maritime University in 1975 and 1977, respectively, and his Ph.D. degree in electronics from the Tokyo Institute of Technology in 1984. He is past-president of the Korea Electromagnetic Engineering Society. Currently, he is a professor of the dept. of radio sciences & engineering at Korea Maritime University. His research interests include the design of microwave circuits and CATV transmission circuits, the development of EM absorbers, and EMC/EMI countermeasures. Prof. Kim is a member of the Institute of Electronics, Information and Communications of Japan, the IEEC of Korea, the KICS, and the KEES. He received the Academy Industry Cooperation(A-I-C) Award from the Korea A-I-C. Foundation in 1990, Treatise Awards from the Korea Electromagnetic Engineering Society and the Korea Institute of Navigation in 1993 and 1998, and the Korea President's Award from the Promotion of Science and Technology in 1995.